INFLUENCE OF ARGON AND BARIUM ION IMPLANTATION ON THE DENSITY OF STATES OF SILICON VALENCE ELECTRONS: EXPERIMENT AND THEORY

B.E. Umirzakov, D.A. Tashmukhamedova, M.B. Yusupjanova*, and B.O. Isakov

Tashkent State Technical University named after Islam Karimov, University Street, 2, Tashkent 100095, Uzbekistan

* *Corresponding author. E-mail: m.yusupjonova@tdtu.uz*

Received: Feb. 06, 2026; Accepted: Jun. 30, 2026

The composition, crystalline, and electronic structure of the Si(111) surface bombarded with low-energy Ar^+ and Ba^+ ions at various doses were studied using scanning electron microscopy, Auger electron spectroscopy, and photoelectron spectroscopy. The following cases will be analyzed: 1) The influence of formation of various chemical bonds on the appearance of new peaks in the photoelectron spectrum. 2) Influence of crystal lattice disorder on the energy positions of the principal spectral peaks of silicon and barium silicides. The analysis reveals that disordering of the Si(111) near-surface region causes a displacement of the main silicon peak by approximately 0.3–0.4 eV, whereas the formation of BaSi and $BaSi_2$ phases induces a more pronounced shift in the range of 0.4-0.5 eV. A simple theory is developed that makes it possible to explain the results on the change in the density of state of the valence band electrons.

Keywords: electronic structure, ion bombardment, photoelectron spectroscopy, chemical bonds, crystal lattice, silicides, composition, dose, valence electrons, annealing

http://dx.doi.org/10.6180/jase.202610_33.050

1. Introduction

In recent years, there has been a significant increase in interest in the fabrication and investigation of nanoscale multilayer semiconductor heterostructures and their physical properties. These nanostructures exhibit strong potential for the fabrication of ultra-highfrequency (UHF) transistors and diodes, optical resonators, as well as electronic and magnetic memory devices, in addition to serving as ohmic contacts and barrier layers in nanoscale systems [1–8]. Low-energy ion bombardment has emerged as a highly efficient and controllable technique for the nanoscale engineering and functional modification of material surfaces and near-surface regions in a broad spectrum of material systems [9–14]. It has been found that the band gap width E_g in nanocrystalline phases of metal silicides, depending on their volumes, can vary within $0.6 - 1$eV.

It is well established that low-energy ion implantation in materials involves a range of processes that induce substantial modifications in both the crystal lattice and electronic structure, ultimately leading to pronounced changes in the physicochemical properties of the surface and near-surface layers [9–14]. In semiconductors, these effects primarily include the generation of structural defects and disordering of the near-surface region, the formation of chemical bonds between semiconductor atoms and implanted dopants, and the emergence of new allowed electronic states within the band gap. All these changes are mainly caused by a change in the stoichiometric composition and phase structure of the near-surface layer. Any alteration in the physicochemical state of a material surface induced by ion implantation including the generation of vacancies and interstitials, impurity incorporation or substitution, the emergence of

electronically active centers, and compound formation - is directly reflected in the experimental photoelectron spectra through systematic variations in peak shape, intensity, and binding energy, the appearance of additional spectral features, and modifications to the overall photoelectron energy distribution.

In this regard, theoretical and experimental studies of the influence of various effects on the change in the electronic structure of materials of various natures have been intensively carried out in recent years [15–25]. In particular, the density of states of valence electrons for Si samples is studied and theoretically founded using the Green's function in [15]. The distribution of electron state densities within the band gap of microcrystalline hydrogenated silicon films ($\mu c - Si : H$) with varying levels of boron doping was investigated using photomodulation spectroscopy [22]. The analysis provided the distribution of electron state densities in both the upper and lower regions of the band gap of $\mu c - Si : H$.

The electronic energy structure of boron nitride in sphalerite (c-BN) and wurtzite (w-BN) crystal lattices was computed using the local coherent potential method combined with the cluster variant of the MT approximation, within the formalism of multiple scattering theory [23]. Using local density functional theory, the authors of [26] computed the self-consistent valence electron densities for CaO crystals with a rock salt lattice, CaF_2 with a fluorite lattice, K_2O with an antifluorite lattice, and their respective constituent sublattices. The results demonstrated that, for crystals possessing distinct Bravais sublattices, the anion sublattice forms a covalently bonded framework into which the metal sublattice is embedded.

The valence-band density of states of an n -GaAs layer formed on an n -GaAs surface via Ar^+ion irradiation at $E_i = 2500$eV was investigated using photoelectron spectroscopy [27]. Several distinct features were observed near the valence-band edge within the binding energy range $E_v < 1.2$eV. The number and positions of these features are in agreement with theoretically predicted quantum confinement levels for a hole quantum well at the surface, with a width comparable to the ion penetration depth ($R_p \approx 3.6$ nm). Additionally, electronic transitions from these confined states to the conduction-band minimum were detected in the characteristic energy-loss spectra of electrons reflected from the surface. Together, these results provide strong evidence that Ar^+ion irradiation induces the formation of a surface quantum well in n -GaAs. Furthermore, the authors of [28] performed density functional theory (DFT) calculations of the band structure and density of states for the diluted magnetic semiconductor $Ga_{1-x}Mn_xAs$.

Computer modeling was used to study, analyze, and obtain new data on the scattering of low-energy ions by a pure InGaP $(001) < 110 >$ multicomponent single crystal under incident ion bombardment in [29, 30]. Effective original algorithms and computer codes for the abovementioned ion-impact processes were developed and created.

We have previously [31–33] experimentally studied the effects of ion bombardment on the electronic structure of Si, Ge and CaF_2. It has been established that, in all cases, disordering of surface layers and the formation of new compounds result in pronounced changes in the structure of photoelectron energy distribution curves.

Consequently, the effects of low-energy ion bombardment on the composition, structure, and properties of various semiconductors have been extensively investigated [31–33]. However, these studies have not specifically isolated the influence of surface layer disordering and new compound formation on the valence electron density of states in Si , or in other singlecrystal materials, under ion irradiation. Moreover, there remains a lack of reliable theoretical interpretation linking the observed modifications in experimental photoelectron spectra to underlying electronic structure changes. In the present study, for the first time, the impact of surface layer disordering and chemical bond formation on the valence electron density of states of silicon during Ba^+ion implantation has been experimentally investigated, and the obtained results are supported by theoretical calculations.

2. Experimental methodology

The object of the research is a single-crystal $Si(111)$ of p-type. Disordering of the $Si(111)$ surface was induced by Ar^+ion bombardment at an energy of $E_0 = 1$keV, with the ion dose varied over the range of 5×10^{13} to 8×10^{16} cm^{-2}. The Ar^+bombardment is carried out perpendicular to the surface. Barium titanate (BaTi) tablets are used as a source of barium ions. After heating at $T = 1100$ K, Ba atoms (vapors) evaporate from the tablet surface and fall on the surface of the hot tungsten spiral, forming Ba^+ions that are directed perpendicularly to the Si surface. The Ba^+ion current is 0.1μ A, and the beam diameter is ~ 2 mm (current density $j = 2 \cdot 10^{13}$ ion $/cm^2$). The method of ultraviolet photoelectron spectroscopy (UPES) was employed to investigate the changes in the density of valence electron states of $Si(111)$ under ion bombardment. The UPES are recorded using gas discharge lamps (in particular, hydrogen lamps). The surface composition of the studied samples is controlled by Auger electron spectroscopy. The spectra are recorded on a 4-grid analyzer with a retarding field. The

analyzer resolution is $\sim 0.1 - 0.2\%$. Ion bombardment and all subsequent measurements were conducted within the same experimental setup at room temperature, under a high vacuum of at least 10^{-7} Pa [34].

3. Result discussions

1. Influence of near-surface layer disordering on the valence electron spectrum of Si(111).

The studies were conducted on Si (111) samples after the surface was cleaned using a standard technique: annealing at $T = 1200$ K for 10 hours, followed by short annealing at $T = 1500$ K were performed until the total concentration of carbon and oxygen decreased to $0.5 - 1$at.%.

During this process, no features characteristic of C and O were detected in the Auger-electron spectra. Si (111) samples were bombarded with Ar^+ions at $E_o = 1$keV, with the dose varying from 0 to 6×10^{16} cm^{-2}. The energy distribution curves of photoelectrons is shown in Fig. 1.

The changes in the position and profile of the main Si A peak were analyzed. Within the ion dose range of D = 0 to 10^{15} cm^{-2}, the peak shifts toward higher binding energies, accompanied by slight broadening. Further increases in the ion dose do not induce significant alterations in the energy distribution curves (EDC). Because Ar^+ions do not alter the surface composition, the observed modifications in the energy distribution curves (EDC) can be ascribed to disordering within the ion-implanted near-surface layers. Apparently, at a dose of 6×10^{15} cm^{-2}, the near-surface layers become completely amorphized, and an "amorphous halo" is observed in the high-energy electron diffraction (HEED) pattern (inset of Fig. 1).

Fig. 2 shows the dependence of the shift of peak A on the dose of Ar^+ions. It can be seen that the maximum shift ΔE is approximately $0.4 - 0.45$eV.

We will attempt to explain these experimental results from a theoretical perspective. The main factor in implantation, as well as doping, affecting the energy spectrum of the single crystal is its disordering. In both cases, the amorphization of the material can be mathematically described by introducing a random field acting on the valence electrons

The electron Green's function $\hat{G}(k, k')$ satisfies the Schrödinger equation:

$$\widehat{G}_{kk'} = G_0(k)\delta_{kk'} + G_0(k)\sum \widehat{V}_{kk'}\widehat{G}_{k'k} \qquad (1)$$

where $\hat{V}_{kk'}$ is a random potential describing the field variation caused by the amorphization of the material, $\delta(x - x') = \delta\left(\bar{x} - \overline{x'}\right)\delta_{\sigma\sigma'} \cdot K$ is the quasi-momentum describing the valence band of Si(111) before ion bombardment, and K' - describes the band of Si after ion bombardment. δ - is the Dirac delta function expressing the energy conservation law during photon absorption.

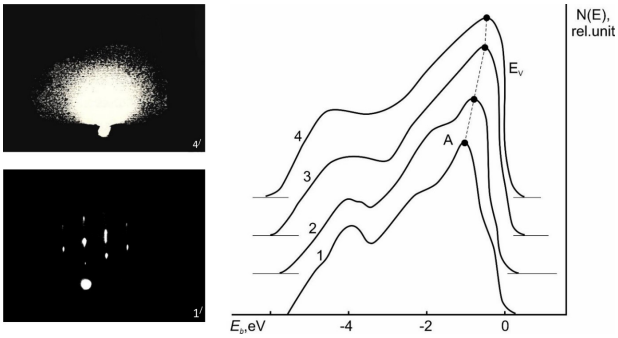

Fig. 1. Photoelectron spectra of Si(111) samples implanted with Ar^+ions at an energy of 1 keV for varying ion doses (D, cm^{-2}) : 1) 0, 2)2×10^{14}, 3) 6×10^{15}, 4) 6×10^{16}, measured at $h\nu = 10.8$eV. The inset shows the high-energy electron diffraction (HEED) patterns of clean Si(111) surfaces and of Si following Ar^+ion bombardment at $E_0 = 1$keV with a dose of 6×10^{15} cm^{-2}, illustrating the structural modifications induced by ion implantation.

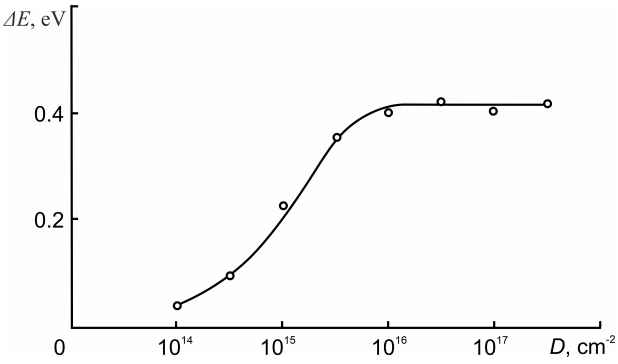

Fig. 2. Dependence of the shift of peak A on the dose of Ar^+ions for Si(111) bombarded with Ar^+ions at $E_o = 1$keV.

Equation (1) describes the random distribution of impurities. Averaging the equation, we obtain:

$$\langle G \rangle = G'_{kk'} = G_0(k) + G_0(k)M_{kk}G'_{kk} \qquad (2)$$

Equation (2) defines the Green's function for the valence band of silicon, where M_{kk} denotes the mass operator, corresponding to the averaged effective complex potential experienced by an electron due to randomly distributed atoms. The real part of M_{kk} accounts for the shift of the peak maximum in the density of states, while the imaginary part describes the peak broadening.

The peak shifts associated with disordering are proportional to the average value of the square modulus of the

random potential $|V_{kk}|^2$

$$M_{kk} = N \int \frac{dk''}{(2\pi)^3} \frac{\left\langle \left| \widehat{V}_{kk} \right|^2 \right\rangle}{\varepsilon_k - \varepsilon_{k''}} \tag{3}$$

where N - is the defect concentration. In this case, the energy of the valence band electrons can be written as:

$$\varepsilon'_k = \varepsilon_k + M_{kk} \tag{4}$$

where ε_k and ε'_k are the energies of the valence electron of Si(111) before and after amorphization, respectively.

Estimates show that the shift of the peak position increases linearly up to a dose of about $\sim 10^{15}$ cm^{-2} while for $D \geq 10^{16}$ cm^{-2} the dependence of M_{kk} on D becomes very weak. Theoretical calculations indicate that the maximum value of M_{kk}, the peak shift is approximately ~ 0.4eV, which is in good agreement with relevant experimental results.

2. Change in the density of states of valence electrons of silicon during the formation of silicides.

Fig. 3 shows the energy distribution curves (EDC) of photoelectrons for p-type Si (111) implanted with Ba^+ ions at different doses at $E_0 = 0.5$keV.

It is evident that with increasing irradiation dose D, a shift of the low-energy edge of the spectrum toward lower binding energies is observed, and the high-energy edge (beginning) of the spectrum first (up to a dose of 6×10^{14} cm^{-2}) shifts toward $E_b = 0$, and then (at $D \geq 10^{15}$ cm^{-2}) shifts toward higher binding energies. A noticeable change in the EDC occurs at $D \geq 2 \times 10^{15}$ cm^{-2}.

The change in the structure of the photoelectron EDC is considered based on the change in the position and intensity of the main peak A of silicon. At low doses $\left(D \leq 5 \times 10^{14} \text{ cm}^{-2}\right)$, the concentration of implanted atoms in the near-surface region is very small ($2-3$ at. %), therefore changes in the electronic structure of the semiconductor surface are mainly associated with disturbances in the crystal structure. Already at $D = 6 \times 10^{14}$ cm^{-2}, the surface layers of Si are significantly disordered and the position of peak A shifts by $\sim 0.2-0.3$eV towards E_V. A new peak B appears near the peak A , which is characteristic of Ba + Si compounds at this dose. At $D = 2 \times 10^{15}$ cm^{-2} peak A completely disappears, i.e. complete disordering of the near-surface layers of Si occurs.

The intensity of peak B rapidly increases, and its position shifts toward E_V by $\sim 0.4-0.5$ eV with increasing ion dose. At 6×10^{16} cm^{-2}, the Ba concentration on the surface layers increases to $40-50$ at. %. $\sim 80-90$% of them form a chemical bond with Si atoms of the BaSi and $BaSi_2$ type

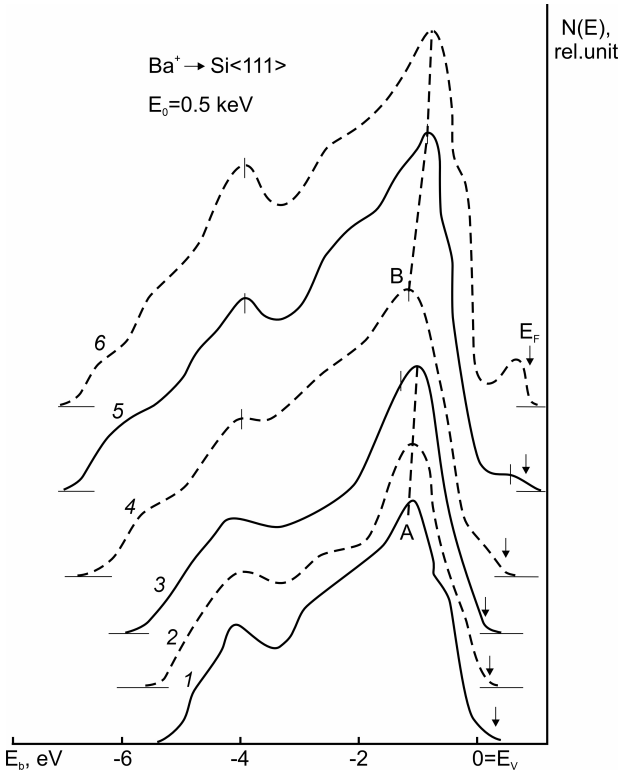

Fig. 3. EDC of photoelectrons for Si (111) implanted with Ba^+ ions with $E_0 = 0.5$keV at D, cm^{-2} : 1) 0; 2) 10^{14}; 3) 6×10^{14}; 4) 2×10^{15}; 5) 8×10^{15}; 6) 6×10^{16}.

[35, 36]. As shown by the experimental data presented in [35, 36], two phases of barium silicides are realized (prove to be stable): BaSi and $BaSi_2$. In both cases, the number of nearest neighbors of barium atoms can be greater than in the case of stoichiometric barium silicide associated with its maximum valence.

The state of an electron in a silicon single crystal is described in the Bloch representation by the Green's function G(W, K), where K is the electron's quasi-momentum in the extended band scheme [37]. In the approximation of independent electrons (the Harty-Fock selfconsistent field approximation), the Green's function is determined by a simple pole expression:

$$G_0(W, K) = \frac{1}{(W - \varepsilon_K + i0)} \tag{5}$$

where ε_K is the electron energy spectrum, determined by solving the Schrödinger equation for an electron in the crystal field of the silicon lattice [38].

When barium ions are implanted into silicon and subjected to subsequent laser or thermal annealing, a new crystalline structure corresponding to the Ba_nSi_m compound is formed. It is important that the chemical bond between bar-

ium and silicon atoms is largely ionic in nature and is carried out by transferring part of the electron charge from the barium atom to the silicon atoms that are its closest neighbors. Although the latter is principally unimportant for the results obtained below, it simplifies the consideration and allows us to neglect the change in the crystal structure in the former approximation and consider that the barium atoms are sources of electrons that pass to the silicon atoms. The change in the crystal structure that occurs during the formation of the compound can, of course, be taken into account by moving to a new Bloch representation that diagonalizes the crystal lattice potential corresponding to the compound formed.

To describe the chemical bond between barium and silicon atoms, it is sufficient to consider two zones numbered by quasi-momenta k and k', where k describes the valence zone of silicon, and k' describes the zone corresponding to the valence electrons of barium. The interaction of these zones is described by the matrix element $V_{kk'}$, corresponding to the probability amplitude of electron transfer from the barium atom to the silicon atom, proportional to the overlap integral of the function.

The state of an electron in the two-band approximation is described by the matrix Green's function $G_{kk'}$, satisfying the Schrödinger integral equation:

$$G_{kk'} = G_0(k)\delta_{kk'} + G_0(k)\sum_{k''} V_{kk''}G_{k''k'}, \tag{6}$$

where k takes two values k and k', corresponding to the bands under consideration. The matrix elements $V_{kk''}$ and $G_{k''k'}$ can be interpreted as the contribution of the self-consistent field caused by the change in the number of electrons on the Si and Ba atoms, which occurs as a result of the electron transfer. In other words, the diagonal matrix elements $V_{kk''}$ and $G_{k''k'}$ describe the "charging" of the silicon and barium atoms, respectively, and determine the degree of ionicity of the resulting compound. It is convenient to include them in the band energies ε_k and $\varepsilon_{k'}$, i.e. to go from ε_k to $\varepsilon_k + V_{kk}$ and from $\varepsilon_{k'}$ to $\varepsilon_{k'} + V_{k'k}$. In what follows, we redesignate ε_k and $\varepsilon_{k'}$ and do not write out the diagonal matrix elements explicitly.

The transition to new values ε_k and $\varepsilon_{k'}$ allows us to describe changes in the position of the displacement of any state of the electron of the valence band, i.e. by changing K we obtain the entire energy spectrum of the valence band, which in turn is displayed on the curve of the energy distribution of the UPES. Further, we focus our attention on the main peaks of the density of states of silicon and barium silicide for certainty.

We are interested in the matrix element of the Green's function G_{KK}, which determines the state of the electron in the valence band of silicon. The expression for this matrix element can be most easily obtained by using the diagram technique [39, 40]. We denote G_{kk} by a line with a thick (bold) arrow ←, the matrix element of the potential $V_{kk'} = V^*_{k'k}$ is denoted by a dotted line, and the free Green's function $G_0(k)$ is represented by a line with a simple arrow ←. As a result, the Green's function G_{kk} is expressed by an infinite series of diagrams representing a geometric progression:

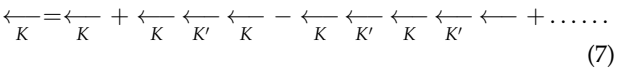

(7)

Summing up this progression, we get

$$\overleftarrow{k} = \frac{1}{(\overleftarrow{k})^{-1} - \overleftarrow{k'}} \tag{8}$$

Using expressions (8), we find:

$$G_{kk} = \frac{W - \varepsilon_{k'}}{((W - \bar{\varepsilon}_k)\cdot(W - \bar{\varepsilon}_{k'}))} \tag{9}$$

$$\text{, where } \bar{\varepsilon}_k = \frac{\varepsilon_k + \varepsilon_{k'}}{2} - \left(\frac{\varepsilon_k - \varepsilon_{k'}}{2}\right)^2 + |V_{kk'}|^2 \tag{10}$$

$$\bar{\varepsilon}_{k'} = \frac{\varepsilon_k + \varepsilon_{k'}}{2} + \left(\frac{\varepsilon_k - \varepsilon_{k'}}{2}\right)^2 + |V_{kk'}|^2 \tag{11}$$

The new value of the energy $\varepsilon_{k'}$, found as a result of solving equation (6), takes into account the change in the energy spectrum of the electrons of the valence band of silicon. According to [40], the degree of covalence of the resulting bond is determined by the expression:

$$\alpha_C = \frac{V_{kk'}}{\sqrt{\left(\frac{\varepsilon_k - \varepsilon_{k'}}{2}\right)^2 + |V_{kk'}|^2}} \tag{12}$$

and the degree of ionicity of the bond

$$\alpha_\Pi = \frac{\varepsilon_{k'} - \varepsilon_k}{\sqrt{\left(\frac{\varepsilon_k - \varepsilon_{k'}}{2}\right)^2 + |V_{kk'}|^2}} \tag{13}$$

The degree of covalence of the bond α_C is proportional to $V_{kk'}$ - the probability amplitude of the electron transition from the barium atom to the silicon atom, and the degree of ionicity of the bond α_Π is proportional to the energy difference $\varepsilon_{k'} - \varepsilon_k$ and contains the contribution $V_{KK} - V_{K'K}$, which describes the self-consistent field of electrons.

The density of electron states of the valence band of silicon:

$$\rho_V(\varepsilon) = \sum \delta(\varepsilon - \bar{\varepsilon}_k) \tag{14}$$

where ε_K is given by formula (10).

The shift of the peak of the density of states of the BaSi compound relative to the corresponding peak of the density of states of silicon is determined by the difference $\varepsilon_{k'} - \varepsilon_k$. Considering the matrix elements $V_{KK'}$, to be small compared to $|\varepsilon_k - \varepsilon_{k'}|$ and expanding formula (10) in a series, limiting ourselves to its first two terms, and taking into account the matrix elements $V_{KK'}$, we find that the shift of the peak due to the formation of a chemical bond is

$$\Delta E = V_{kk} - \left(\frac{|V_{kk'}|^2}{|\varepsilon_k - \varepsilon_{k'}|} \right) \tag{15}$$

The first term in (15) is positive, it takes into account the Coulomb repulsion of electrons on the silicon atom and leads to an increase in the electron energy, i.e. to a decrease in the electron binding energy. This term is related to the ionicity of the compound and prevails over the second term, which determines the covalency of the bond.

The value of $V_{KK'}$ can be estimated using the formula

$$V_{kk'} \sim \frac{1}{\varepsilon} \int \frac{e^2}{|x|} \delta_\Pi(\bar{x}) dx \tag{16}$$

where $e^2/|x|$ is the energy of the Coulomb interaction of electrons, $\delta_\Pi(\bar{x})$ is the distribution of electrons transferred from the Ba atom to the Si atom, ε is the dielectric constant of the crystal. Integration in (16) is carried out over the volume of the Si atom. Thus, we find

$$V_{kk'} \sim \frac{e^2}{\varepsilon a} \delta_\Pi \tag{17}$$

where a is the radius of the atom, δ_Π is the average value of the additional charge coming to one silicon atom ($e^2/a \approx 13.6$eV). The calculated value of V_{KK} is $0.8 \div 1$eV, which is consistent with the magnitude of the observed peak shift. The overlap integral $V_{KK'}$ can be estimated similarly, however, the second term in (15) containing it makes a small contribution.

4. conclusion:

1. For Ba^+ion irradiation, the observed modifications in the valence electron spectrum are attributed to both amorphization of the ion-implanted layers and the formation of $Ba - Si$ compounds. In contrast, the effects of Ar^+ion bombardment on the extent of surface disorder in silicon single crystals and on the valence-band density of states have been systematically investigated experimentally and supported by theoretical analysis. The observed energy shift is approximately 0.4 eV .
2. It has been established that bombardment with Ba^+ions leads to changes in the density of states of $Si(111)$ valence electrons, caused by both the disordering of the near-surface layer and the variation in the composition of the ion-implanted layers.
3. Theoretical and experimental estimates have been made separately for the effects of surface amorphization and Ba silicide formation on the changes in the valence electron density of states.

References

[1] V. Vorobyov, A. Rogov, V. Nuzhdin, V. Valeev, and A. Stepanov, (2020) *"Sputtering of silicon surface during low-energy high-dose implantation with silver ions"* **Technical Physics 65(7): 1156-1162.** DOI: 10.1134/S1063784220070269.

[2] T. Nemoto, S. Aonuki, R. Koitabashi, Y. Yamashita, M. Mesuda, K. Toko, and T. Suemasu, (2021) *"Solar cell operation of sputter-deposited n-$BaSi_2$/p-Si heterojunction diodes and characterization of defects by deep-level transient spectroscopy"* **Appl. Phys. Express 14: 051010.** DOI: 10.35848/1882-0786/abfb87.

[3] R. Gainutdinov, M. Khamadeev, E. Zajtseva, and M. Salakhov, (2012) *"Photon density of states in optical nanomaterials and control of energy levels of atoms"* **Nanosystems: Physics, Chemistry, Mathematics 3(1): 56-63.** URL: https://www.mathnet.ru/eng/nano659.

[4] D. Gromov, O. Pyatilova, S. Bulyarosky, A. Belov, and A. Raskin, (2013) *"Specific features of the formation of arrays of silver clusters from a thin film on a SiO_2 surface"* **Physics of the Solid State 55(3): 619-623.** DOI: 10.1134/S106378341303013X.

[5] K. Hoppe, W. Fahrner, D. Fink, S. Dhamodoran, A. Petrov, A. Chandra, A. Saad, F. Faupel, V. Chakravadhanula, and K. Zaporotchenko, (2008) *"An ion track based approach to nano- and micro-electronics"* **Nucl. Instr. Meth. B. 266: 1642-1646.** DOI: 10.1016/j.nimb.2007.12.069.

[6] D. Tashmukhamedova, M. Yusupjanova, A. Tashatov, and B. Umirzakov, (2018) *"Study of the influence of implanted atoms on the coefficients of the sputtering of silicon and silicon with a thin oxide film"* **Journal of Surface Investigation 12(5): 902-905.** DOI: 10.1134/S1027451018050117.

[7] F. Priolo, T. Gregorkiewicz, M. Galli, and T. Krauss, (2014) *"Silicon nanostructures for photonics and photovoltaics"* **Nature Nanotechnology 9: 19-32.** DOI: 10.1038/nnano.2013.271.

[8] K. Karabeshkin, P. Karaseov, and A. Titov, (2016) *"Effect of an increase in the density of collision cascades on the efficiency of the generation of primary displacements during the ion bombardment of Si"* **Semiconductors 50(8): 989-995.** DOI: 10.1134/S1063782616080145.

[9] S. Donaev, B. Umirzakov, and D. Tashmukhamedova, (2015) *"Electronic structure of $Ga_{1-x}Al_xAs$ nanostructures grown on the GaAs surface by ion implantation"* **Technical Physics 60(10): 1563-1566.** DOI: 10.1134/S1063784215100138.

[10] R. L. Savio, L. Repetto, P. Guida, E. Angeli, G. Firpo, A. Volpe, V. Ierardi, and U. Valbusa, (2016) *"Control of the micrometric scale morphology of silicon nanowires through ion irradiation-induced metal dewetting"* **Solid State Commun 240: 41-45.** DOI: 10.1016/j.ssc.2016.04.023.

[11] D. Tashmukhamedova, (2006) *"Study of composition and electronic structure of $CoSi_2$/Si interface"* **Bulletin of the Russian Academy of Sciences: Physics 70(8), 1409-1411.** URL: https://elibrary.ru/item.asp?id=27854241.

[12] E. Ergashov, D. Tashmukhamedova, F. Djurabekova, and B. Umirzakov, (2016) *"Effect of surface microroughness on the composition and electronic properties of CdTe/Mo(111) films"* **Bulletin of the Russian Academy of Sciences: Physics 80(2): 138-140.** DOI: 10.3103/S1062873816020064.

[13] C.-M. Lee, S.-P. Chang, S.-J. Chang, and C.-I. Wu, (2013) *"Fabrication of high-efficiency silicon solar cells by ion implant process"* **International Journal of Electrochemical Science** *8*(6): 7634–7645. DOI: 10.1016/S1452-3981(23)12832-X.

[14] M. Eisa, J. Conradie, C. Mtshali, N. Mongwaketsi, and M. Maaza, (2026) *"Optimization of ion beam elements using mathematical transport formalism"* **Journal of Applied Science and Engineering 30: 26030027.** DOI: 10.6180/jase.202607_30.027.

[15] M. Guzzo, G. Lani, F. Sottile, P. Romaniello, M. Gatti, J. Kas, J. Rehr, M. Silly, F. Sirotti, and L. Reining, (2011) *"Valence electron photoemission spectrum of semiconductors: Ab Initio description of multiple satellites"* **Phys. Rev. Lett. 107: 166401.** DOI: 10.1103/PhysRevLett.107.166401.

[16] Z. Li, Y. Zhang, L. Ma, G. Tang, G. Wu, and F. Hu, (2022) *"A new explanation on valence electron structure of C, Si, and Ge crystals with diamond structure based on photoelectron spectra"* **Journal of Electron Spectroscopy and Related Phenomena 254: 147153.** DOI: 10.1016/j.elspec.2021.147153.

[17] M. Yusupjanova, D. Tashmukhamedova, and B. Umirzakov, (2016) *"Composition, morphology, and electronic structure of the nanophases created on the SiO_2 Surface by Ar^+ ion bombardment"* **Technical Physics 61, 628-630.** DOI: 10.1134/S1063784216040253.

[18] A. Keqi, M. Gehlmann, G. Conti, S. Nemšák, A. Rattanachata, J. Minár, L. Plucinski, J. Rault, J. Rueff, M. Scarpulla, M. Hategan, G. Pálsson, C. Conlon, D. Eiteneer, A. Saw, A. Gray, K. Kobayashi, S. Ueda, O. Dubon, C. Schneider, and C. Fadley, (2018) *"Electronic structure of the dilute magnetic semiconductor $Ga_{1-x}Mn_xP$ from hard x-ray photoelectron spectroscopy and angle-resolved photoemission"* **Physical Review B. 97(1523): 155149.** DOI: 10.1103/PhysRevB.97.155149.

[19] F. Gygi, (2023) *"All-Electron Plane-Wave Electronic Structure Calculations"* **Journal of Chemical Theory and Computation 19(4): 1300-1309.** DOI: 10.1021/acs.jctc.2c01191.

[20] N. Zikrillaev, K. Iliev, G. Kushiev, S. Isamov, S. Koveshnikov, B. Abdurakhmanov, and B. Isakov, (2026) *"Study of photocells based on Ge_xSi_{1-x} structures"* **Journal of Applied Science and Engineering 29(03): 685-691.** DOI: 10.6180/jase.202603_29(3).0019.

[21] B. Umirzakov, D. Tashmukhamedova, and F. Khudaykulov, (2022) *"Effect of implantation of Ba^+ ions on the composition, electronic and crystal structure of W(111) and WO_2 surfaces"* **Journal of Surface Investigation 16(6): 992-996.** DOI: 10.1134/S1027451022050202.

[22] A. Kazansky and K. Khabarova, (2004) *"Distribution of the density of electronic states in the energy gap of microcrystalline hydrogenated silicon"* **Semiconductors 38(10): 1221-1224.** DOI: 10.1134/1.1808833.

[23] T. Zhdanova, V. Ilyasov, and I. Nikiforov, (2001) *"Specific features of the electronic band structure and X-ray spectra of boron nitride in sphalerite and wurtzite modifications"* **Physics of the Solid State 43(8): 1445-1448.** DOI: 10.1134/1.1395081.

[24] O. Yastrubchak, N. Tataryn, L. Gluba, S. Mamykin, J. Sadowski, T. Andrearczyk, J. Domagala, O. Kondratenko, V. Romanyuk, O. Fedchenko, Y. Lytvynenko, O. Tkach, D. Vasilyev, S. Babenkov, K. Medjanik, K. Gas, M. Sawicki, T. Wosinski, G. Schönhense,

and H.-J. Elmers, (2023) *"Influence of Bi doping on the electronic structure of (Ga,Mn)As epitaxial layers"* **Sci Rep. 13: 17278.** DOI: 10.1038/s41598-023-43702-w.

[25] M. Sumiya, S. Ueda, K. Fukuda, Y. Asai, Y. Cho, L. Sang, A. Uedono, T. Sekiguchi, T. Onuma, and T. Honda, (2018) *"Valence band edge tail states and band gap defect levels of GaN bulk and $In_xGa_{1-x}N$ films detected by hard X-ray photoemission and photothermal deflection spectroscopy"* **Appl. Phys. Express 11: 021002.** DOI: 10.7567/APEX.11.021002.

[26] Y. Zhuravlev and A. Poplavnoy, (2003) *"The distribution of the valence electron density in predominantly ionic crystals with different Bravais sublattices"* **Physics of the Solid State 45(1): 36-40.** DOI: 10.1134/1.1537406.

[27] V. Mikushkin, (2018) *"Quantum well on the n-GaAs surface irradiated by argon ions"* **JETP Letters 107(4): 243-246.** DOI: 10.1134/S0021364018040094.

[28] V. Yarzhemsky, S. Murashov, and A. Izotov, (2019) *"Electronic structure and ferromagnetic transition temperature of $Ga_{1-x}Mn_xAs$ in the nonempirical local exchange method"* **Inorganic Materials 55: 1-8.** DOI: 10.1134/S0020168519010187.

[29] M. Karimov, U. Kutliev, S. Bobojonova, and K. Otabaeva, (2021) *"Investigation of angular spectrum of scattered inert gas ions from the InGaP (001) surface"* **Physics and Chemistry of Solid State 22(4): 742-745.** DOI: 10.15330/pcss.22.4.742-745.

[30] U. Kutliev, M. Otabaev, M. Karimov, F. Masharipov, and I. Woiciechowski, (2023) *"Scattering of low-energy Ne^+ ions from the stepped surface of InGaP(001)<110> at the small angles of incidence"* **Physics and Chemistry of Solid State 24(3): 542-548.** DOI: 10.15330/pcss.24.3.542-548.

[31] B. Umirzakov and S. Donaev, (2017) *"On the creation of ordered nuclei by ion bombardment for obtaining nanoscale Si structures on the surface of CaF_2 films"* **Journal of Surface Investigation 11: 746-748.** DOI: 10.1134/S1027451017040139.

[32] B. Umirzakov, D. Tashmukhamedova, M. Ruzibaeva, F. Djurabekova, and S. Danaev, (2014) *"Investigation of change of the composition and structure of the CaF_2/Si films surface at the low-energy bombardment"* **Nuclear Instruments and Methods in Physics Research Section B: Beam Interactions with Materials and Atoms 326: 322-325.** DOI: 10.1016/j.nimb.2013.10.094.

[33] S. Abraeva, D. Tashmukhamedova, S. Gulyamova, M. Yusupjanova, and A. Xujaniyazova, (2023) *"Impact of bombardment by Ar^+, Na^+ and O_2^+ ions on spectra of elastically scattered electrons of single-crystal Ge"* **E3S Web of Conferences 401: 05006.** DOI: 10.1051/e3sconf/202340105006.

[34] D. Tashmukhamedova and M. Yusupjanova, (2021) *"Formation of nanoscale structures on the surface of MgO films upon bombardment with low-energy ions"* **Journal of Surface Investigation 15(5): 1054-1057.** DOI: 10.1134/S1027451021050402.

[35] D. Tashmukhamedova, B. Umirzakov, and M. Mirzhalilova, (2004) *"Structure and properties of nanocrystals grown in near-surface ranges of Si and GaAs by low-energy ion implantation"* **Izvestiya Akademii Nauk. Ser. Fizicheskaya 68(3): 424-427. (in Russian)**: URL: https://www.elibrary.ru/item.asp?id=17641066.

[36] K. Boltaev, D. Tashmukhamedova, and B. Umirzakov, (2014) *"Structure and electronic properties of nanoscale phases and nanofilms of metal silicides produced by ion implantation in combination with annealing"* **Journal of Surface Investigation 8(2): 326-331.** DOI: 10.1134/S1027451014010108.

[37] K. S. Thorne and R. D. Blandford. *Statistical Physics: Volume 1 of Modern Classical Physics*. Princeton University Press, 2021. URL: https://press.princeton.edu/books/paperback/9780691206127/statistical-physics.

[38] K. W. Böer and U. W. Pohl. *Semiconductor physics*. Springer Nature, 2023. URL: https://link.springer.com/referencework/10.1007/978-3-031-18286-0.

[39] F. Kugler, (2018) *"Counting Feynman diagrams via many-body relations"* **Phys. Rev. E. 98: 023303.** DOI: 10.1103/PhysRevE.98.023303.

[40] R. M. Martin. *Electronic structure: basic theory and practical methods*. Cambridge University Press, 2020. DOI: 10.1017/9781108555586.